

Shape Modification with Expansive Cement Concrete for Confinement with FRP Composites

by Z. Yan, C.P. Pantelides, and L.D. Reaveley

Synopsis: To improve the confinement effectiveness of FRP composites for square and rectangular columns, shape modification is performed by using prefabricated FRP shells combined with expansive cement concrete. Chemical post-tensioning using expansive cement concrete is used to change the FRP confinement from “passive” to “active”. Experimental results are presented demonstrating the effectiveness of this method. An analytical stress-strain model is developed for shape-modified FRP-confined columns with expansive cement concrete which is based on the modified Willam-Warnke plasticity model, the Popovics general stress-strain concrete model, and the dilatancy behavior obtained from the present study. This model is implemented by an incremental approach which accounts for the variable FRP confinement during the loading process. The analytical results show satisfactory agreement with the experiments.

Keywords: chemical post-tensioning; confinement; expansive cement concrete; FRP composites; stress-strain behavior

1048 Yan et al.

Zihan Yan is a structural engineer for Nishkian Meninger, San Francisco, CA. He received his PhD from University of Utah, Salt Lake City, Utah. His research interests include strengthening of concrete with fiber-reinforced polymer composites, and structural diagnostics and rehabilitation of reinforced concrete building and construction.

ACI member **Chris P. Pantelides** is a professor of civil and environmental engineering at the University of Utah. He is a member of ACI Committee 374, Performance-Based Seismic Design of Concrete Buildings. His research interests include seismic design, evaluation, and rehabilitation of reinforced concrete building and bridge construction.

ACI member **Lawrence D. Reaveley** is a professor of civil and environmental engineering at the University of Utah. He is a member of ACI Committee 369, Seismic Repair and Rehabilitation. His research interests include the areas of performance-based structural engineering and the rehabilitation of existing structures.

INTRODUCTION

Fiber Reinforced Polymer (FRP) composites have been used in the retrofit of concrete columns to improve their capacity, displacement ductility or both. It is well-known that FRP composite jackets can provide effective lateral confinement for circular concrete columns, and substantially enhance their axial strength and ultimate axial strain; however, FRP confinement is much less effective for square and rectangular columns compared to circular columns. This observation has been verified in tests performed by Rochette and Labossière (2000) and Pessiki et al. (2001). The reason for this is that FRP composite jackets resist axial loads by membrane action, and are more effective for circular sections as opposed to square or rectangular column sections with corners and long flat sides; stress concentrations at the corners and inefficient confinement at the flat sides cause loss of membrane action of the FRP composite and reduction of confinement. Because of the presence of steel ties, rounding of the corner radius in existing square/rectangular columns is limited. In addition, lower FRP confinement effectiveness results in softening behavior for square and rectangular columns and the FRP composite ruptures prematurely; therefore, the high strength of FRP composite materials cannot be fully utilized.

A possible approach to increasing the effectiveness of FRP-confined rectangular columns is to perform shape-modification that is to modify the column cross-section into an elliptical, oval, or circular section. One method for performing shape-modification is to use prefabricated (non-bonded) FRP composite shells combined with expansive cement concrete. For this method, a prefabricated elliptical/oval/circular FRP shell may be used as stay-in-place formwork for casting additional expansive cement concrete around the square or rectangular section to achieve shape modification. The advantage of using expansive cement concrete is that a post-tensioning effect could be achieved on the FRP composite shell through chemical post-tensioning, which would in turn improve the compressive behavior of concrete columns. Expansive cement consists of a Portland

cement component and a calcium-sulfoaluminate anhydrite component; the hydration of the latter component causes expansion. This material has been used since 1960 for making chemically prestressed concrete. Klein et al. (1961) investigated the properties of expansive cement for chemical post-tensioning and found that factors influencing the magnitude and rate of the expansive reaction include: chemical composition of components, proportions of the two components in the total cementing material, richness of mix, conditions of curing, and degree of restraint. Benuska et al. (1971) further studied the curing effects on expansion and mechanical behavior of expansive cement concrete; their tests showed that expansive cement concrete was very good for prefabricated elements or structural elements and systems in which the optimum amount of chemical prestress required was relatively low.

The mechanism of expansive cement concrete is used with FRP composite shells for confinement enhancement. When expansive cement concrete is applied to prefabricated FRP shells, expansion of the cement grout is restrained by the FRP shell; the FRP composite is stressed in tension, thus creating a post-tensioning effect. It is obvious that this post-tensioning effect would increase the confinement behavior of FRP jackets and change the confinement action from “passive” to “active”.

In this paper, an experimental program was conducted for studying shape modification of square/rectangular specimens confined with FRP composites. Two FRP composite systems, a Carbon Fiber Reinforced Polymer (CFRP) system and a Glass Fiber Reinforced Polymer (GFRP) system were used. Column shape modification was performed by using prefabricated FRP composite shells with expansive cement concrete. Test results are presented regarding failure modes and the stress-strain behavior; comparison is made between shape-modified specimens and specimens without shape modification.

This paper also presents an analytical stress-strain model for the shape-modified concrete column with the FRP composite shell and expansive cement concrete. As a part of this research, a plasticity model based on the Willam-Warnke (1975) plasticity concrete model was developed to account for the axial strength of FRP-confined concrete. Conclusions regarding the effectiveness of the shape modification method with expansive cement concrete and its practical implementation are made.

RESEARCH SIGNIFICANCE

Confinement of concrete utilizing shape modification of square and rectangular columns with post-tensioned non-bonded FRP composite shells and expansive cement concrete is investigated. Square and rectangular sections were modified into circular and elliptical sections; post-tensioning of the FRP composite shells reduces corner effects, and enhances membrane action and confinement effectiveness. It is shown that expansive cement concrete is an efficient method for post-tensioning FRP composite shells and modifying the FRP confinement from passive to active. The proposed analytical model shows a good agreement with the experimental results.

EXPERIMENTAL PROGRAM**Specimens**

The experimental program involved three groups of specimens: S, R2 and R3; “S” denotes a series of square specimens; “R2” and “R3” denote a series of rectangular specimens with cross-sectional aspect ratio of 2:1 and 3:1, respectively. All specimens were 914 mm high; no steel reinforcement was used inside the concrete. Each group included an unconfined (baseline) specimen, two specimens with the original cross-section confined by CFRP or GFRP composites, and two shape-modified specimens by using prefabricated CFRP or GFRP shells and expansive cement concrete. Table 1 lists the details of all specimens; the identification of the specimens, as shown in Table 1, uses a three-code base. The first part of the code is the shape of the column (Square or Rectangular), and the aspect ratio of the rectangular cross-section (2:1 or 3:1). The second part of the code indicates the type of FRP composite (CFRP or GFRP) and the number of layers (2 or 6). The third part denotes the type of material used to achieve shape modification (E denotes Expansive cement concrete and 0 denotes no shape modification, i.e. the specimen has the original square or rectangular geometry). The modified cross-section of the original square specimen was circular and the modified cross-section of the original rectangular specimen was elliptical; the cross-sectional aspect ratio was close to the original prior to shape modification.

Material properties

Two types of concrete were used in this study: regular concrete and expansive cement concrete. Regular concrete was used to cast the original specimens; expansive cement concrete was used to perform the shape modification. The concrete compressive strength for the original specimens was 15 MPa. The expansive cement used in this research was Type-K and Komponent. The two principal constituents of Komponent are calcium sulfoaluminate and gypsum or calcium sulfate. The formation of ettringite crystals, which result from hydration of the two ingredients, is what causes the expansion. When expansion is restrained, for example by a pre-fabricated FRP composite shell, expansive cement concrete induces tensile stresses in the FRP composite shell that cause chemical “post-tensioning”. The mix design for the expansive cement concrete is listed in Table 2. The compressive strength of the expansive cement concrete after 28 days was 10 MPa.

Two FRP composite materials were used to confine the concrete columns. One was *SikaWrap Hex 103C* which is a high strength, unidirectional carbon fiber fabric with epoxy resin. The other was *Aquawrap G-06*, which is a unidirectional pre-impregnated glass fiber fabric with urethane resin. Both FRP composite materials were cured at ambient temperature conditions. The material properties determined from tensile coupon tests, per ASTM Standard D3039, are shown in Table 3.

For shape-modified specimens, prefabricated FRP composite shells were made prior to casting of expansive cement concrete. Strain gauges were installed on the FRP composite at midheight of the specimens and a data acquisition system was used to measure the hoop expansion of the FRP composite shells during the curing period of the expansive cement concrete. Figure 1 shows the measured FRP hoop strain versus time

starting at casting of the expansive cement concrete. The FRP hoop strain approached a constant value after 60 days and this asymptotic value is defined as the initial hoop strain $\varepsilon_{j,ini}$, which refers to the state before axial load is applied. The initial hoop strain $\varepsilon_{j,ini}$ depends on the aspect ratio B_j/D_j of the prefabricated FRP shells, which is defined as the length of the major axis, B_j , to the length of the minor axis, D_j , of the elliptical cross-section. In general, circular jackets achieved the highest expansion while the elliptical shell with the highest aspect ratio had the smallest expansion. Also, GFRP shells achieved a higher expansion compared to CFRP shells. These observations can be visualized from Fig. 2 for the relationship between $\varepsilon_{j,ini}$ and the aspect ratio. From Fig. 2, the proposed relationship between $\varepsilon_{j,ini}$ and B_j/D_j for FRP shells with 2 CFRP layers is:

$$\varepsilon_{j,ini} = 0.0020 - 0.00041 \left(\frac{B_j}{D_j} \right) \quad (1)$$

and for FRP shells with 6 GFRP layers is:

$$\varepsilon_{j,ini} = 0.0025 - 0.00041 \left(\frac{B_j}{D_j} \right) \quad (2)$$

Loading and instrumentation

All specimens were subjected to a monotonic uniaxial load until failure under displacement control with a constant loading rate of 1.3 mm per minute. The tests were performed using a 9 MN actuator with a stroke of 0.6 m. Two Linear Variable Differential Transducers (LVDTs) were installed to measure axial compressive strains; strain gauges were used to measure the transverse strains over the circumference of the cross-section.

EXPERIMENTAL RESULTS AND DISCUSSION

Failure modes

For FRP-confined square/rectangular specimens without shape modification, failure typically starts with concrete crushing followed by fracture of the FRP composite jacket. In rectangular and square sections, FRP breakage appeared at one of the corners, in a small area near the column midheight; a concrete cone was seen after peeling the broken FRP composite jacket. The failure was brittle due to the presence of the corner and flat side effects, which eliminate membrane action of the FRP jacket and result in weaker confinement. Figure 3(a) shows the typical failure mode for the FRP-confined specimen with the bonded FRP jacket.

In contrast to specimens with bonded FRP jackets, the failure of shape-modified specimens with non-bonded FRP shells and expansive cement concrete was fracture of the FRP jackets first, followed by cracking of the expansive cement concrete and concrete core. FRP breakage extended over the entire height of the column, showing the extensive participation of the FRP jacket in confinement. At the end of the test, most

specimens remained in one piece, and shear and compression cracks were seen in the expansive cement concrete. Figure 3(b) shows the typical failure mode for a shape-modified specimen with non-bonded FRP shells and expansive cement concrete. Specimens with non-bonded FRP shells and expansive cement concrete had a higher strain ductility compared to specimens with bonded FRP jackets, demonstrating the higher effectiveness of the post-tensioned FRP shells. The degree of damage of shape-modified specimens with non-bonded FRP shells and expansive cement concrete varied with aspect ratio. Specimens with a smaller aspect ratio reached a higher capacity and a higher degree of damage.

Axial stress-strain response

Figure 4 presents the axial stress versus axial strain response for each group, including the baseline specimens and the specimens confined with CFRP composite jackets. The axial displacements were measured using the average of two LVDTs, and the axial stress was computed by dividing the axial compression load by the cross-sectional area. It is seen that CFRP-confined square specimen S-C2-0 showed a limited hardening behavior and both CFRP-confined rectangular specimens R2-C2-0 and R3-C2-0 demonstrated a softening behavior; a drop of axial stress was observed after the initial axial strength was reached, and the degree of softening increased as the aspect ratio increased. For shape-modified specimens, the stress-strain curves show ascending branches without softening behavior. In some cases, the initial slope of the stress-strain curve for shape-modified specimens is less than that of specimens without shape modification. This is because the unconfined compressive strength of expansive cement concrete was smaller than that of regular concrete, and the membrane effect from the FRP composite shell was not significant in the initial phase of axial loading. Similar observations were made for GFRP-confined specimens, as shown in Fig. 5. It is also noted from Fig. 5(c) that very limited increases as well as the limited hardening behavior were obtained for shape-modified specimen R3-G6-E compared to the specimen confined with the bonded FRP jacket, R3-G6-0, showing that the GFRP composite is more sensitive to the cross-sectional aspect ratio.

To characterize the stress-strain behavior of FRP-confined concrete columns, three important parameters are identified: axial strength, ultimate axial strain, and ductility ratio μ , as shown in Table 4. The ductility ratio is used to evaluate the ductility performance of FRP-confined concrete and is calculated as the ratio of the total area under the stress-strain curve to the area bounded by a slope of the initial elastic stiffness and the plastic plateau (Rochette and Labossière 2000); for specimens with hardening behavior the plastic plateau passes through the unconfined concrete strength f_{co}' ; for specimens with softening behavior the plastic plateau passes through the peak axial strength f_{cc}' . In Table 4, the volumetric ratio of the FRP composite jacket for each specimen ρ_{FRP} is also presented; ρ_{FRP} is the ratio of the area of the FRP composite jacket to the cross-sectional area of the concrete specimen.

It can be seen from Figs. 4, 5 and Table 4 that the shape-modified specimens showed significant increases in axial strength, ultimate axial strain, and ductility. However, the level of improvement of the compressive behavior depends on the aspect ratio. As seen from Figs. 4 and 5, the improvement is significant for shape-modified square specimens S-C2-E and S-G6-E since their modified shape was circular; the improvement was less significant for shape-modified rectangular specimens R3-C2-E and R3-G6-E with the higher aspect ratio; this means that the effect of shape modification is reduced as the section becomes a flatter ellipse. Therefore, to improve the confinement effectiveness, a lower aspect ratio after shape modification is preferred, in the form of an oval shape. However, the practical use of a prefabricated FRP shell with a low aspect ratio such as an oval shape always increases the modified cross-sectional area by a large amount of concrete, and possible foundation issues resulting in cost increases.

Effective FRP confinement ratio

For FRP-confined concrete circular or elliptical columns, the FRP confining stress f_l can be expressed as:

$$f_l = \frac{1}{2} \rho_{FRP} E_j \varepsilon_j \quad (3)$$

where ρ_{FRP} = FRP volumetric ratio; E_j = elastic modulus of FRP composite, and ε_j = FRP hoop strain for circular cross-sections or average FRP hoop strain for elliptical cross-sections, defined as the average of the hoop strain at the minor and major axis (Yan 2005). The effective confinement ratio $\frac{f_{lu}}{f_{co}}$ is defined as the ratio of the ultimate FRP confining pressure f_{lu} at rupture of the FRP jacket to the unconfined concrete strength f_{co} ; for shape-modified columns, f_{co} is obtained by calculating the mean unconfined compressive strength over the modified cross-section. The general form of the ultimate FRP confining pressure f_{lu} for circular or elliptical columns can be expressed as:

$$f_{lu} = \frac{1}{2} \rho_{FRP} E_j k_\varepsilon \varepsilon_{fu} \quad (4)$$

where k_ε = FRP jacket efficiency factor; and ε_{fu} = ultimate FRP tensile strain obtained from material coupon tests. In Eq. (4), k_ε is used to account for the reduction factor of the FRP ultimate hoop strain compared to the material coupon tests and depends on the aspect ratio of the cross-section. Since the FRP composite shells are already post-tensioned prior to axial loading, k_ε is smaller than that of the corresponding bonded FRP jackets. Based on this study, k_ε was found to be in the range of 0.30 and 0.50 for circular non-bonded FRP shells, and a value of 0.40 is recommended; for elliptical cross-sections, k_ε is controlled by the aspect ratio as (Yan 2005):

$$k_\varepsilon = 0.15 \left(1 + \left(\frac{B_j}{D_j} \right)^{-0.65} \right) \frac{B_j}{D_j} \geq 1.5 \quad (5)$$

The effective confinement ratio $\frac{f_{lu}'}{f_{co}}$ is also an indication of the trend of the stress-strain behavior; the authors suggest that the FRP-confined column shows a strain hardening behavior when $\frac{f_{lu}'}{f_{co}}$ is larger than 0.2 and a strain softening behavior when $\frac{f_{lu}'}{f_{co}}$ is smaller than 0.2 (Yan 2005).

Dilatancy behavior of shape-modified columns

In this study, the dilatancy behavior of FRP-confined concrete is represented by the volumetric strain versus axial strain relationship. Volumetric strain ϵ_v is defined as the FRP area strain in the two transverse orthogonal directions minus the axial strain in the concrete column ϵ_c :

$$\epsilon_v = 2\epsilon_j - \epsilon_c \tag{6}$$

where ϵ_j is defined as the FRP hoop strain for circular cross-sections or average FRP hoop strain for elliptical cross-sections. Figure 6 shows the volumetric strain versus axial strain relations for shape-modified specimens with expansive cement concrete. Since the FRP shell was already post-tensioned prior to axial loading through chemical post-tensioning, the amount of radial expansion was smaller compared to bonded FRP jackets. Therefore, the axial strain was larger than the hoop area strain, $2\epsilon_j$; this reveals that the axial strain was dominant in the volumetric strain versus axial strain curve. This dilatancy behavior is extremely important for shape-modified FRP specimens with expansive cement concrete because in this case the FRP confinement becomes “active” instead of “passive”.

From Fig. 6, the relationship between volumetric strain and axial strain is approximately linear and α is the slope of a straight line that is:

$$\epsilon_v = -\alpha\epsilon_c \tag{7}$$

where α is determined by the FRP confinement ratio $\frac{f_{lu}'}{f_{co}}$ and is proposed as (Yan 2005)

$$\alpha = 0.26 + 0.428 \frac{f_{lu}'}{f_{co}} \tag{8}$$

ANALYTICAL MODEL

Modified Willam-Warnke (MWW) model for FRP-confined concrete

Prediction of the axial strength is based on the ultimate surface described by Willam and Warnke (1975), as shown in Fig. 7(a); σ_1 , σ_2 , and σ_3 are the three stress components. For FRP-confined concrete, σ_1 is taken as the axial compressive stress; σ_2 and σ_3 represent the confining stress provided by the FRP composite in the two transverse orthogonal directions. In plasticity theory the sign convention is that

compressive stress is negative. Figure 7(b) shows the projection of the ultimate surface on the $\overline{\sigma}_a - \overline{\tau}_a$ plane, where $\overline{\sigma}_a$ = normalized mean normal stress and $\overline{\tau}_a$ = normalized mean shear stress, as expressed in Eqs. (10) and (11) in terms of $\sigma_1, \sigma_2, \sigma_3$, and the unconfined concrete strength f_{co}' .

$$\overline{\sigma}_a = \frac{\sigma_1 + \sigma_2 + \sigma_3}{3f_{co}'} \tag{9}$$

$$\overline{\tau}_a = \frac{1}{\sqrt{15}f_{co}'} [(\sigma_1 - \sigma_2)^2 + (\sigma_2 - \sigma_3)^2 + (\sigma_3 - \sigma_1)^2] \tag{10}$$

As shown in Fig. 7(b), the compression meridian is a second-order parabola and can be expressed as (Willam and Warnke 1975):

$$\overline{\tau}_a = b_0 + b_1 \overline{\sigma}_a + b_2 \overline{\sigma}_a^2 \tag{11}$$

where b_0, b_1 , and b_2 are material constants obtained from experiments. From the FRP-confined column tests performed by the authors (Yan 2005) these values are: $b_0 = 0.0417, b_1 = -0.7955$ and $b_2 = -0.1041$. For specimens with hardening behavior, the axial strength f_{cc}' is achieved when the FRP confining pressure f_l reaches its maximum f_{lu} . Therefore, $\sigma_1 = -f_{cc}'$; $\sigma_2 = \sigma_3 = -f_{lu}$ at the ultimate state. Substituting the corresponding terms in Eqs. (9), (10), and (11) and solving this equation system gives the axial strength f_{cc}' for the range of $\frac{f_{lu}'}{f_{co}'} \geq 0.2$:

$$f_{cc}' = \left(-4.322 + 4.721 \sqrt{1 + 4.193 \frac{f_{lu}'}{f_{co}'} - 2 \frac{f_{lu}'}{f_{co}'}} \right) f_{co}'; \quad \frac{f_{lu}'}{f_{co}'} \geq 0.2 \tag{12}$$

For the range of $\frac{f_{lu}'}{f_{co}'} < 0.2$, the authors suggest the axial strength f_{cc}' as (Yan 2005):

$$f_{cc}' = \max \left(\left(\frac{-4.322 + 4.721 \sqrt{1 + 4.193 \frac{f_{lu}'}{f_{co}'} - 2 \frac{f_{lu}'}{f_{co}'}}}{0.0768 \ln \left(\frac{f_{lu}'}{f_{co}'} \right) + 1.122} \right) f_{co}', f_{co}' \right); \quad \frac{f_{lu}'}{f_{co}'} < 0.2 \tag{13}$$

Analytical stress-strain relationship

The Popovics (1973) model was used for developing the analytical stress-strain relationship for shape-modified specimens with expansive cement concrete. This model describes the ascending stress-strain relation up to the peak point, as shown in Fig. 8 and is thus suitable for the shape-modified specimen with hardening behavior. An analytical model for shape-modified specimens with softening behavior has also been developed and is described elsewhere (Yan 2005). The analytical expression of Popovics (1973) is based on the relationship between axial stress f_c and axial strain ϵ_c expressed as:

$$f_c = \frac{E_0 \varepsilon_c}{1 + (K - 1) \left(\frac{\varepsilon_c}{\varepsilon_{cc}'} \right)^r} \tag{14}$$

where E_0 = initial elastic modulus and E_s = secant modulus at the peak stress given as:

$$E_s = \frac{f_{cc}'}{\varepsilon_{cc}'} \tag{15}$$

and shown in Fig. 8. The parameters K and r are defined as:

$$K = \frac{E_0}{E_s} = E_0 \frac{f_{cc}'}{\varepsilon_{cc}'} \tag{16}$$

$$r = \frac{K}{K - 1} \tag{17}$$

Parameter ε_{cc}' is the ultimate axial strain proposed by Imran (1994) as:

$$\frac{\varepsilon_{cc}'}{\varepsilon_{co}'} = 6 \left(\frac{f_{cc}'}{f_{co}'} - 0.8 \right) \tag{18}$$

where ε_{co}' is the axial strain corresponding to the axial strength of the unconfined concrete f_{co}' ; for regular concrete, ε_{co}' is set to 0.002 mm/mm.

Traditional steel-confined concrete models, i.e. the Mander et al. model (1988), assume a constant confining pressure which is based on the assumption that the confining device has yielded and behaves in a perfectly plastic manner, thus providing a constant confining pressure. However, this assumption is inappropriate for FRP confinement because the confining pressure provided by FRP jackets or shells, f_l , varies continuously and exhibits an approximately linear behavior until failure (Moran and Pantelides 2002). Therefore, the analytical FRP-confined concrete model must be developed based on an incremental approach to account for the variable FRP confining pressure f_l . In the proposed procedure, the axial loading is divided into a number of steps i . The detailed analytical approach is described as follows:

Based on the given information such as the cross-sectional dimensions, material properties, and the number of FRP composite layers, the effective confinement ratio f_{lr}/f_{co}' and the dilatancy parameter α can be obtained from Eqs. (4) and (8) respectively. For each step i , an incremental FRP hoop strain $\Delta\varepsilon_j$ is applied and the current hoop strain ε_j^i is calculated by accumulating the incremental hoop strain $\Delta\varepsilon_j$ up to the current load step as: $\varepsilon_j^i = \sum_{k=1}^i \Delta\varepsilon_j^k$ (superscript i attached to the variables indicates the load step at which the variables are updated). Then the current axial strain ε_c^i is obtained from Eqs. (6) and (7) corresponding to an FRP hoop strain ε_j^i by using the

dilatancy parameter α . The confining pressure f_l^i can be obtained from Eq. (3) corresponding to an FRP hoop strain ε_j^i . Therefore, by setting $f_{lu} = f_l^i$ the maximum axial stress, f_{cc}^i at ε_j^i can be calculated from the model of Eq. (12) for $\frac{f_{lu}}{f_{co}} \geq 0.2$ or Eq (13) for $\frac{f_{lu}}{f_{co}} < 0.2$. The relationship between the current axial strain ε_c^i and axial stress f_c^i , which corresponds to the current hoop strain ε_j^i can be obtained by using the Popovics model of Eqs. (14) - (18). The incremental steps are repeated until the hoop strain ε_j^i reaches its ultimate state $\varepsilon_{ju} = k_\varepsilon \varepsilon_{fu}$, as shown in Eq. (4). For circular FRP composite shells k_ε is set equal to 0.4; for elliptical shells, Eq. (5) should be used for calculating k_ε .

The incremental approach is easily implemented using a spreadsheet or any computer program. Figure 9 shows comparisons between the analytical model and experimental results; it can be seen that the analytical results agree well with the experiments.

CONCLUSIONS

Shape modification by using expansive cement concrete and prefabricated FRP composite shells can restore the membrane effect in FRP composite confinement of square and rectangular concrete columns; it can change the FRP confinement from “passive” to “active”, and thus achieve a higher axial strength for square and rectangular columns compared to the original columns with the same number of FRP composite layers. For lightly or moderately FRP-confined square or rectangular columns, the shape modification method could modify the stress-strain behavior from softening to hardening and therefore achieve a higher strength and ductility. The experimental results showed that the effectiveness of shape modification depends largely on the aspect ratio of the modified section: the optimal column shape for FRP confinement is the circular cross-section; for rectangular columns, especially those with a large aspect ratio, change to a circular section requires a large volume of expansive cement concrete and possible modifications to the foundation. Therefore, for strengthening rectangular columns by shape modification, the influence of factors such as volume increase, increase in surface area, and required strength, ductility, and ultimate strain need to be considered to obtain an optimal solution.

The proposed analytical stress-strain model for shape-modified FRP-confined columns with expansive cement concrete is based on the modified Willam-Warke (1975) plasticity model, the Popovics general stress-strain (1973) concrete model, and the dilatancy behavior obtained from the present study. This model is implemented by an incremental approach which accounts for the variable FRP confinement during the

loading process. The analytical results show satisfactory agreement with the experiments

ACKNOWLEDGMENTS

The authors would like to acknowledge the contributions of FRP composite materials by Sika and Air Logistics and the contribution of Type K cement and Komponent from CTS Company. The financial support provided by the Utah Department of Transportation is also acknowledged.

REFERENCES

- Benuska, K. L., Bertero, V. V., and Polivka, M. (1971). "Self-Stressed Concrete for Precast Building Units." *PCI Journal*, March-April 1971, 72-84.
- Imran, I. (1994). "Application of Non-Associated Plasticity in Modeling the Mechanical Response of Concrete." *Ph.D. Dissertation*, University of Toronto, 1994.
- Klein, A., Karby, T., and Polivka, M. (1961). "Properties of An Expansive Cement for Chemical post-tensioning." *ACI Journal, Proceedings*, Vol. 58, No. 1, July 1961, 59-82.
- Moran, D. A., and Pantelides, C. P. (2002). "Variable Strain Ductility Ratio for Fiber Reinforced Polymer-Confined Concrete." *Journal of Composites for Construction*, ASCE, 2002, 6(4), 224-232.
- Pessiki, S., Harries, K. A., Kestner, J. T., Sause, R., and Ricles, J. M. (2001). "Axial Behavior of Reinforced Concrete Columns Confined with FRP Jackets." *Journal of Composites for Construction*, ASCE, 2001, 5(4), 237-245.
- Popovics, S. (1973). "Numerical Approach to the Complete Stress-Strain Relation for Concrete." *Cement Concrete*, 1973, 3(5), 583-99.
- Rochette, P., and Labossière, P. (2000). "Axial Testing of Rectangular Column Models Confined with Composites." *Journal of Composites for Construction*, ASCE, 2000, 4(3), 129-136.
- Willam, K. J., and Warnke, E. P. (1975). "Constitutive Model for the Triaxial Behavior of Concrete." *Proceedings, International Association for Bridge and Structural Engineering*, Vol. 19, 1-30.
- Yan, Z. (2005). "Shape Modification of Rectangular Columns Confined with FRP Composites." *Ph.D. Dissertation*, Department of Civil and Environmental Engineering, University of Utah, Salt Lake City, Utah, May 2005.

Table 1—Details of column specimens

Group	Specimen	Cross- section before shape modification (mm)	Length of major axis after shape modification (mm)	Length of minor axis after shape modification (mm)	Aspect ratio	FRP type and number of FRP layers
S	S-0-0	279×279	-	-	1:1 ⁽¹⁾	Unconfined
	S-C2-0	279×279	-	-	1:1 ⁽¹⁾	2L CFRP
	S-G6-0	279×279	-	-	1:1 ⁽¹⁾	6L GFRP
	S-C2-E	279×279	406	406	1:1 ⁽²⁾	2L CFRP
	S-G6-E	279×279	406	406	1:1 ⁽²⁾	6L GFRP
R2	R2-0-0	203×381	-	-	2:1 ⁽³⁾	Unconfined
	R2-C2-0	203×381	-	-	2:1 ⁽³⁾	2L CFRP
	R2-G6-0	203×381	-	-	2:1 ⁽³⁾	6L GFRP
	R2-C2-E	203×381	648	368	1.8:1 ⁽⁴⁾	2L CFRP
	R2-G6-E	203×381	660	362	1.8:1 ⁽⁴⁾	6L GFRP
R3	R3-0-0	152×457	-	-	3:1 ⁽³⁾	Unconfined
	R3-C2-0	152×457	-	-	3:1 ⁽³⁾	2L CFRP
	R3-G6-0	152×457	-	-	3:1 ⁽³⁾	6L GFRP
	R3-C2-E	152×457	775	279	2.8:1 ⁽⁴⁾	2L CFRP
	R3-G6-E	152×457	762	298	2.6:1 ⁽⁴⁾	6L GFRP

⁽¹⁾ Square cross-section, ⁽²⁾ Circular cross-section, ⁽³⁾ Rectangular cross-section, ⁽⁴⁾ Elliptical cross-section.

Table 2—Mix design per m³ of expansive cement concrete

Property		Weight (KN)	Volume (m ³)
CEMENT	TYPE K EXPANSIVE CEMENT	2.20	0.07
	COMPONENT	1.04	0.03
WATER	WEIGHT/VOLUME	2.34	0.24
ROCK	ASTM C-33 (SSD) 10mm PEA GRAVEL	3.26	0.13
SAND	ASTM C-33 (SSD)	13.42	0.53

Table 3—Material properties of CFRP and GFRP composites

FRP Composite	Tensile Strength (MPa)	Tensile Modulus (MPa)	Tensile Strain (mm/mm)	Ply Thickness (mm)
CFRP	1220	8.69×10 ⁴	0.014	1.0
GFRP	228	1.69×10 ⁴	0.014	1.6

Table 4—Experimental results

Group	Specimen	ρ (%)	$f_{cc}'(f_{co}')^*$ (MPa)	ϵ_{cu}' (mm/mm)	μ
S	S-0-0	-	15.2	0.002	0.90
	S-C2-0	2.55	26.2	0.010	1.15
	S-G6-0	11.64	22.1	0.020	0.93
	S-C2-E	1.80	49.1	0.022	2.38
	S-G6-E	8.00	44.4	0.021	2.03
R2	R2-0-0	-	14.8	0.002	0.90
	R2-C2-0	2.68	24.1	0.023	1.14
	R2-G6-0	12.27	21.9	0.021	0.91
	R2-C2-E	1.50	27.4	0.011	1.69
	R2-G6-E	7.10	31.2	0.018	2.72
R3	R3-0-0	-	14.6	0.002	0.90
	R3-C2-0	3.11	21.6	0.021	0.78
	R3-G6-0	14.22	21.6	0.021	0.89
	R3-C2-E	1.80	25.6	0.008	1.45
	R3-G6-E	8.00	22.8	0.021	0.93

* f_{co}' = compressive strength of unconfined concrete specimens: S-0-0, R2-0-0 and R3-0-0; f_{cc}' = axial strength of FRP-confined concrete specimens.

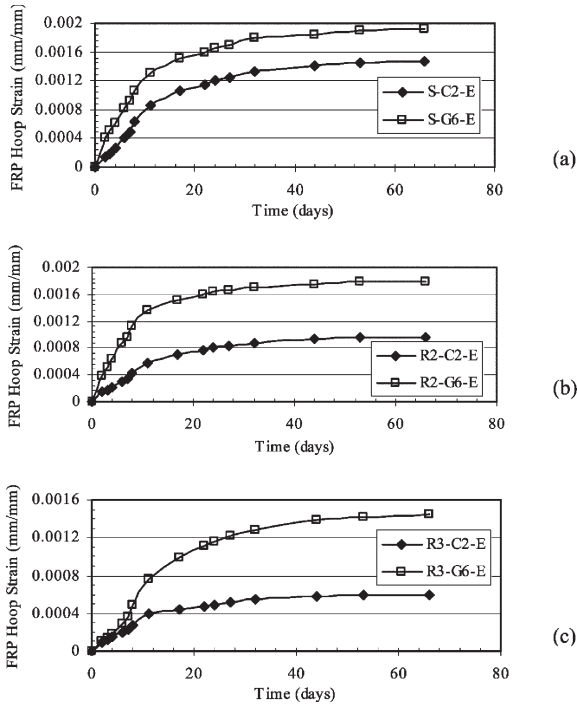


Figure 1 – Expansion history for FRP shells with expansive cement concrete: (a) Square S; (b) Rectangular R2; (c) Rectangular R3.

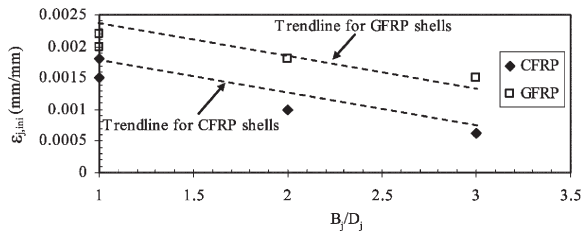


Figure 2 – Relationship between aspect ratio $\frac{B_j}{D_j}$ and initial hoop strain $\epsilon_{j,ini}$.

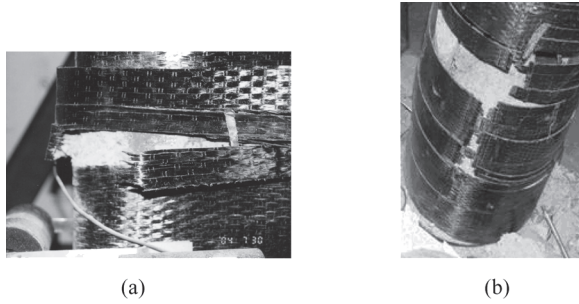


Figure 3 – Typical failure modes for FRP-confined specimens: (a) without shape modification; (b) with shape modification.

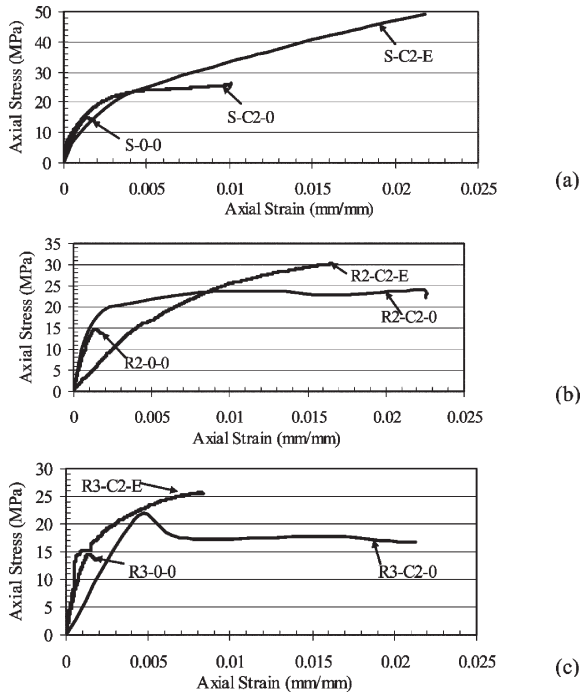


Figure 4 – Axial stress-strain curves for CFRP-confined columns: (a) Square S; (b) Rectangular R2; (c) Rectangular R3.

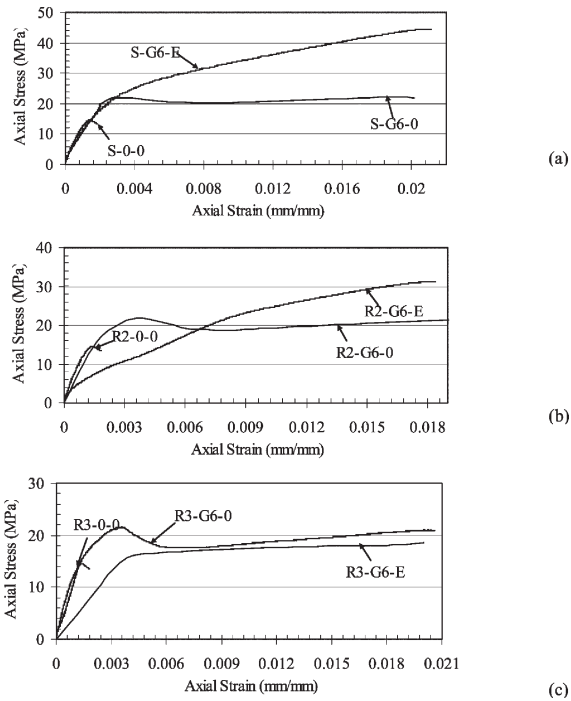


Figure 5 – Axial stress-strain curves for GFRP-confined columns:
(a) Square S; (b) Rectangular R2; (c) Rectangular R3.

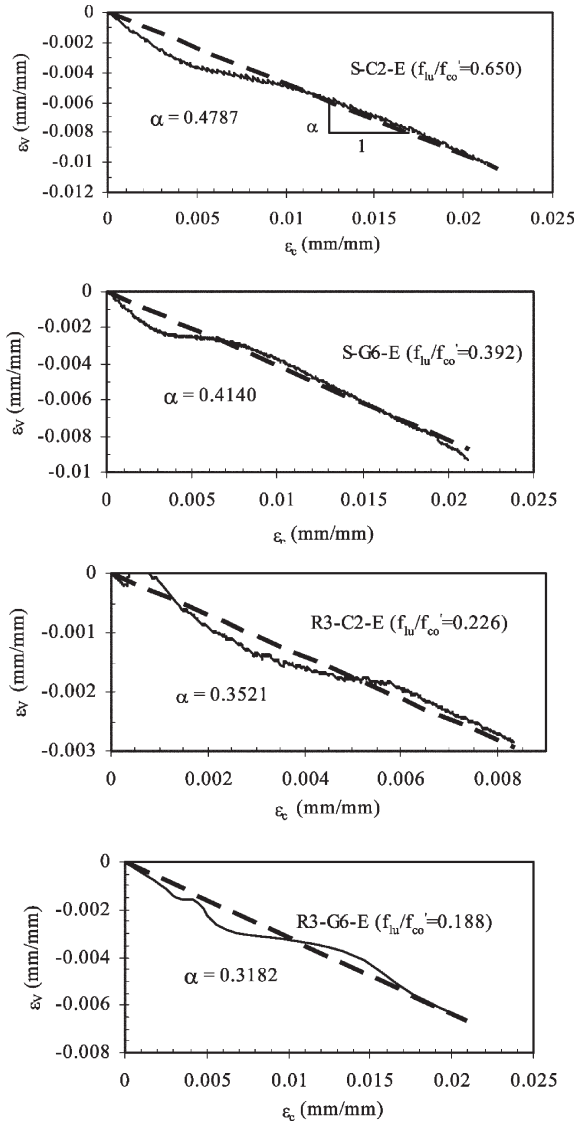


Figure 6 – Volumetric versus axial strain relationships for shape-modified specimens with expansive cement concrete.

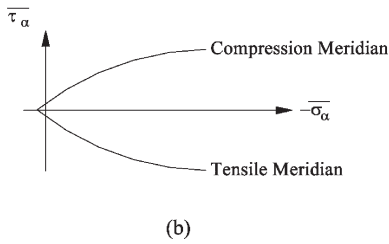
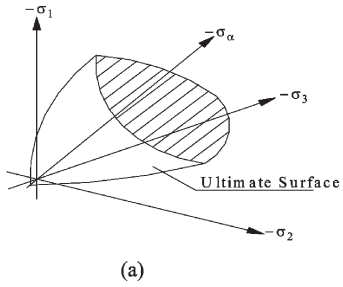


Figure 7 – Willam-Warke plasticity model: (a) 3D view; (b) meridian section on $\sigma_a - \tau_a$ plane.

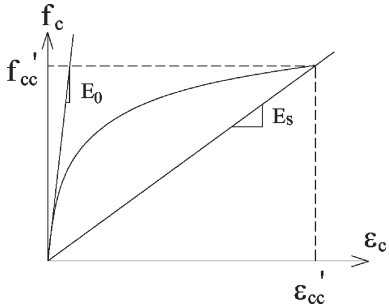


Figure 8 – Axial stress-strain curve for specimens with hardening behavior.

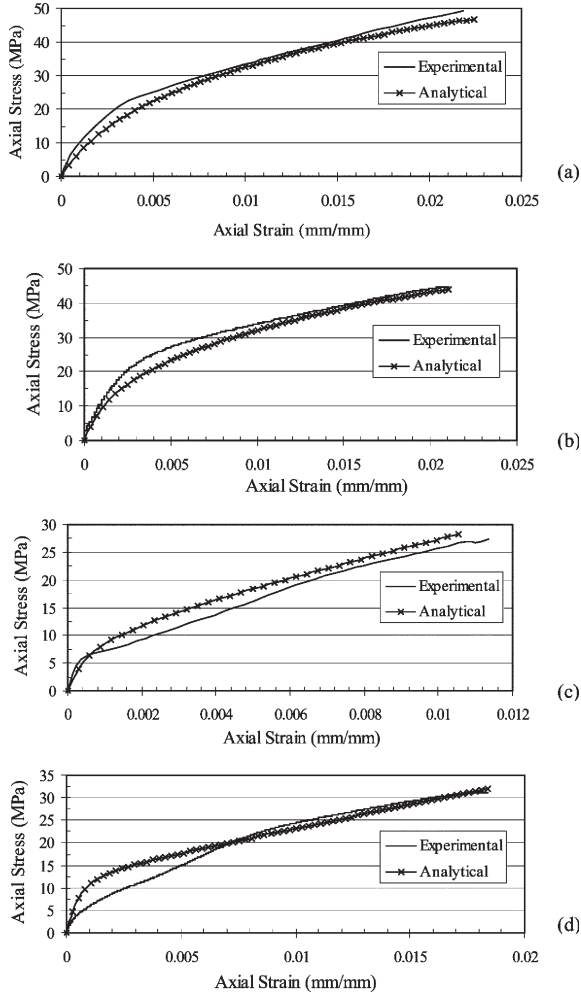


Figure 9 – Comparisons between analytical results and experiments: (a) S-C2-E; (b) S-G6-E; (c) R2-C2-E; (d) R2-G6-E.